Flow Study on the ESS target water model

K.Haga[1], Y.Takeda, G. Bauer / Paul Scherrer Institute
B. Guttek / Forschungzentrum Jülich

INTRODUCTION

The liquid target of ESS has a configuration of horizontal channel flow. The target container is partitioned into two channels, the lower one is for inflow and the upper one for outflow. The liquid turns at the end where the proton beam is impinging. Detail is given elsewhere [1].

For this configuration, the behaviour of flow in these channels and turning pocket is very important for a secured heat transport out of the reaction zone. Since the flow is bent in the most critical region, occurrence of any recirculation in this region may lead to a boiling of mercury.

The hydrodynamic study is under way to investigate experimentally general behavior of the flow in the configuration of ESS liquid target. The study was performed by two-dimensional model and three dimensional mock up test is under progress. The liquid used is water at this stage. The mercury experiment is under preparation.

We always start the investigation of this kind by using a two-dimensional (2D) model with water. This is because of easiness of preparation and handling the liquid, for enabling flow visualization technique to be used, and good for understanding the flow phenomena.

In this paper the results of 3D experiment is mainly given, while the results of 2D experiment is briefly presented, since all the work and detail of the results can be found elsewhere [2].

Two-dimensional Model

Experimental set-up

Flow measurement for flow mapping was made using ultrasound Doppler method [3,4]. This technique has been developed at PSI for the target R & D program, and we established the method to obtain two-dimensional-two-components (2D2C) velocity vector filed. [5].

The test section, as illustrated in Fig.1, is made of plexiglas, 55 cm long, 20 cm wide and 10 cm height, which follows an entry region of ca. 100 cm. At the position of 3 cm high from the bottom plate a separation plate (2 mm thickness) is placed. An inflow liquid flows in a lower channel (30 mm x 200 mm channel cross sectional area) toward the hemicylindrical top (radius 50 mm) and after bending 180° there, it flows out in an upper channel (70 mm x 200 mm area). This test section is set in a water loop which has a maximum flow rate of ca. 2 *l*/s. The one measurement was focused on the recirculation zone in the upper channel, while the other on the returning flow in the hemicylindrical top. Ultrasound transducers are assembled in special mounting devices, which are attached to the outer wall of the test section. For the measurement of the upper channel, eight transducers are mounted in a block with a regular separation distance of 15 mm having a constant inclination angle of 15° to the normal line. Together with the measurements where the inclination angle is changed to -15°, we have 96 velocity profiles, from which we can form a two dimensional vector field. For the measurement of hemicylindrical region, 14 transducers are set with 12° separation angle and with constant inclination of 15°to the normal line on and at the outer wall. This configuration generates 28 velocity profiles. (on the method for the flow

[1] On leave from JAERI

mapping, ref [5].) More detail of the experimental setup and experimental method can be found in [5].

Flow map

The vector field obtained (361 vectors) is given in Fig. 2 for the upper channel. It is clearly seen that a flow is recirculating in the lower part of the channel (on the separation plate). On the two lowest lines, directions of vector are leftward for X<210 and rightward beyond this point, although vectors are quite small. On the third lowest line, it is more clearly seen that it flows leftward with significant velocity levels, ca. 10 cm/s. The thickness (height) of the recirculation zone is ca. 30 mm at x=50 mm and it extends to the point x=ca.200 mm (250 mm from the top of the cylinder). Beyond this point, the flow is more or less parallel and directed to the exit and no structure was seen.

Fig. 3 shows a result of the measurement for the hemicylindrical region, where 705 vectors are plotted. This shows clearly a returning flow along the end wall as generally anticipated. Since we plotted only time average velocity field, the flow is smooth and no significant small structure is displayed.

Spanwise motion

From the UVP measurements as well as from visual observation, we found that a spanwise motion is not negligibly small. The velocity profiles of the spanwise direction were measured at the top position of the hemicylindrical part along the wall. The Fig. 4 is a time averaged profile. It shows clearly a large spanwise circulation; a pair of large vortices which is observed from the result that the flow direction is opposite from the center of the channel toward outside. By using the orthogonal decomposition of the space-time velocity profile, we found that there are four rolls to the spanwise direction. There is a large scale motion forming one pair of large vortices and secondary two pairs of vortices, which are superposed to the larger one. It is yet to be studied whether this roll structure is intrinsic in this flow configuration or due to an inflow condition of this experimental setup.

Three-dimensional Model

Experimental set-up

Fig.5 shows the water loop used in this experiment. Water is supplied to the test section through three inlet channels. Flow meters are installed at each inlet pipes and the flow rates are regulated by the valves below the flow meters. The maximum achievable total flow rate is 2.5 L/s with the present system. Electrodes for electrolysis are also installed just above the flow meters to generate tiny gas bubbles that makes seeding better for UVP.

Fig.6 shows a cut-out view of ESS model showing the interior geometry. The manifold is made of stainless steal to be used in mercury experiments in future. Three lower pipes are the inlets of water and the upper one the outlet. The rectangular flange seen in the middle allows insertion of the gas injector system to simulate the gas injection into mercury for the pressure wave attenuation, which was not used in this study. Several projections fixed on the outlet pipe are reinforcements to sustain the weight of the manifold.

The model was made with plexiglass which also enables UVP measurement as well as flow visualization experiments. To minimize the reflection effect of ultrasound within the wall, the wall thickness was made thin to be 3mm. The outer width of the model is 306mm. The height is 156mm at the rear edge and 106mm at the front. The window has a round shape with the radius

of 53mm at the center. The side walls are also rounded. Fig.7 shows the flow direction of water in the model. Water flows into three channels of the model through three inlet pipes of the manifold. Two of the channels are placed at the side of the model, and one is at the bottom. The experimental results obtained with the two dimensional model showed the tendency that the recirculation region becomes larger and stronger as the inlet flow rate from the bottom channel is increased. The two additional side channels were installed with intention of making the recirculation region small while keeping the enough cooling of the target window. They are also expected to shift the recirculation region out of the reaction zone. The water passing through the side channels flow into the main channel of the target at the front edge. Three water flows collide each other inside the target window so that the flow structure must be very complicated there. Thereafter the water flows backward to the outlet.

Flow Vector Mapping

The vector maps we can obtain is a time averaged flow field in the model. The flow vector components are calculated with average velocity profiles of 1024 profiles on each measuring lines. It takes about 90 seconds to collect the data of 1024 velocity profiles for one measuring line. Designing an arrangement of measuring lines is important for flow mapping. The angle of the measuring lines to the line normal to the surface of the model must be less than the critical angle of 32.9 degrees, while the distribution of the crossing points should cover whole the flow field of interest. Fig.8 shows a typical arrangement of the measuring lines used in this experiment. True velocity vectors are obtained at 193 crossing points on one plane. These measuring lines are inclined 10 degrees right and left to the perpendicular line, which makes the crossing angle between two measuring lines as 20 degrees. Four perpendicular measuring lines placed on both sides cross with slanted measuring lines at the angle of 10 degrees. These angles were determined to minimise the reflection effect. The maximum depth of the vector field from the top of the target window is 30cm.

Experiment Conditions

Table 1 shows the experiment conditions. One data set corresponds to one vector map. There are 22 data sets with different combinations of flow rate and the height of measuring plane. The MP height in the second column means the height of measuring plane. The base level is at the center of the model, as is shown in Fig.9, and the MP height is expressed by the height from the base level. The MP angle in the third column is the inclination of the measuring plane to horizon, that means, the MP angle of 0 degree corresponds to a horizontal measuring plane. The data sets from Nr.1 to Nr.6 are trial cases to decide the best measuring line arrangement. After the measuring line arrangement was decided as Nr.7, the measurement of the flow field was started systematically. The flow velocity fields in the horizontal plane were measured at three different heights. The items, A, B, C in the flow rate column correspond to the inlet channels as is shown in Fig.7. The ratio of flow rates of three inlet channels were changed as 1:0:1, 2:1:2, 1:1:1, 1:2:1, 0:1:0 with keeping the total flow rate constant at 0.88L/s. Flow velocity at the front edge means the average water velocity at the exit of each channels. The last data set, Nr.22, is of the measuring plane inclined 10 degrees upward.

Experimental Results

It should be noted that the flow velocity vectors shown here are the projection of real vectors to the measuring plane. Since the flow structure is highly three dimensional, the water flow in the model cannot be expressed perfectly on a two dimensional plane, but the general behavior of the total flow can be understood with two dimensional vector maps.

Comparison of vector maps of different flow rate ratios at the base level

The vector fields obtained with the data set Nr.9,11 and 7 are shown in Fig.10, 11, and 12. These data sets can be compared to know the change of a flow field with a relative increase of the lower channel (channel B). The recirculation region can be clearly seen on both sides of the center line in all of these cases. The flow direction at the center line is slightly shifted and inclined to the right, which makes the recirculation region on the left side larger. The reason of the asymmetry flow is not clear; it depends on the accuracy of the flow meter of inlet channels, the symmetry of the target window, or the inlet flow condition. When the flow rate of channel B is small (Fig.10), the recirculation region is small and the flow velocity is also small, which means the flow in these region is almost stagnant. The left side recirculation region begins from the depth of ca. 90mm and continues to ca. 200mm. As the flow rate of channel B increases (Fig.11 and 12), the recirculation region becomes larger and stronger. The starting depth of the region is almost the same with the case of Fig.10, but the end depth extends to ca. 300mm in Fig.11 and further (undetectable) in Fig.12. Fig.13 shows the profile of x component of flow velocity along the x-axis ($V_x(x)$). This shows the peculiar pattern of one dimensional velocity profile across the channel. The plot indicates that there are two counter-rotating vortices along the x-axis, and it also indicates that the border between the two vortices is shifted to the right of the center line. In the case of equal inlet flow rate, the peak of V_x is small compared to the case of large flow rate of B channel, which shows the vortex became weak. In the case of small B channel flow rate, the sign of V_x is opposite to other two cases on the right side, which shows the contraction of vortex, that is, the center of the vortex shifted crossing the x-axis and the flow direction on the x-axis was reversed.

Comparison of vector maps at different levels with equal flow rates

The vector fields obtained with the data set Nr.15 and 18 are shown in Fig.14 and 15. Together with the Fig.11, the vector maps at equal flow rates can be observed at different level. The flow going to the center from side channels just inside the target window become strong as the measuring plane goes up. This shows the flow from side channels is directed upward by the flow from channel B. The flow at the center line is inclined to the right also in these cases. The recirculation region on the left side begins from the depth of ca. 50mm in Fig.15 and it shifts backward in Fig.11 and 14, which indicates that the recirculation region is three dimensional and the interface between the recirculation region and the stream going back in the main channel is inclined. A small vortex seems to be generated behind the edge of the side channels.

Comparison of vector maps of different levels with the inlet flow from bottom channel

Fig.16, 17 and 18 show the flow field in which water was supplied only through the bottom channel. This is the same case with the experiment of two dimensional model. The large vectors inside the target window in Fig.18 correspond to the direct stream from the bottom channel. The vectors near the center line of the model show there is a backward stream in the upper measuring plane. As the measuring plane goes down, the backward stream disappears in Fig.16 and 17 and only the frontward and sideward stream becomes dominant. This shows there is a large vertical recirculation ranging from the bottom to the top of the main channel, just the same with the flow observed in two dimensional model. But in this case, the side wall is rounded and it generates spanwise flow making the total flow field more complicated.

CONCLUSIONS

Using water as the model fluid, average flow behavior in the ESS target model was studied experimentally by UVP method for 2D and 3D structures.

In 2D experiments, it was found that a large recirculation zone is generated in the upper flow channel where most of the beam energy is deposited. It consists of two counterrotating vorticies, but the spanwise motion is relatively small compared to the axial motion. The shape and size of the vortices are supposed to be dependent on flow geometry and flow conditions of the target liquid.

The ESS target geometry has three inlet channels generating cross-flow on the surface of the target window, which was expected to prevent the creation of the recirculation region in the main channel or at least to reduce the effect. But, the results of the 3D mockup water experiments showed that the recirculation region is still generated on the reaction zone with a more complicated flow pattern, at least, under the low flow rate conditions applied here. A pair of recirculation are observed on both sides of the center line of the model. Since the shape of two counterrotating vortices is clearer and spanwise motion is stronger than in 2D model, they are considered to be generated by the side channel flows. As the flow rate ratio of three inlet channels changed, the size and intensity of the recirculation region also changed, but it never disappears. It would be expected that different pattern of flow fields may appear with higher flow rates, but generally the large vortex structure seen with the low flow rate does not change even with higher flow rate. In order to decide the optimum target geometry and flow conditions, further studies have to be done experimentally and numerically.

Reference

[1] H. Lengeler, Ed., Third General ESS-Meeting, Baden, March 22-25, 1995, ESS 5-24-M

[2] Y. Takeda, T. Dury, and G.S. Bauer, "Liquid metal target for spallation neutron sources" Proc. of NURETH-8, Vol.2, pp1252 (1997)

[3] Y. Takeda, Velocity profile measurement by ultrasonic Doppler method, Exp. Therm. & Fluid Sci., 10, 444-453, (1995)

[4] Y.Takeda, Ed., First International Symposium on Ultrasonic Doppler Methods for Fluid Mechanics and Fluid Engineering, PSI, Switzerland, 9.-11. Sept., 1996

[5] H. Kikura & Y. Takeda, ASME Fluid Engineering Division, Summer Meeting, Washington DC, July 98

Table 1 Experimental Conditions for the Water Experiments of the ESS Target Model

Data-Set Nr.	MP Height [mm]	MP Angle [deg]	Flow Rate [L/s]				Velocity at the Front Edge [mm/s]			ML Set Nr.
			A	B	C	Total	A	B	C	
1	0	0	0.33	0.33	0.33	0.99	456	413	456	1
2	0	0	0.33	0.33	0.33	0.99	456	413	456	2
3	0	0	0.33	0.33	0.33	0.99	456	413	456	3
4	0	0	0.33	0.33	0.33	0.99	456	413	456	4
5	0	0	0.33	0.66	0.33	1.32	456	825	456	5
6	0	0	0.22	0.22	0.22	0.66	304	275	304	6
7	0	0	0.22	0.44	0.22	0.88	304	550	304	7
8	0	0	0.44	0	0.44	0.88	608	0	608	7
9	0	0	0.35	0.18	0.35	0.88	483	225	483	7
10	0	0	0	0.88	0	0.88	0	1100	0	7
11	0	0	0.29	0.29	0.29	0.88	401	363	401	7
12	+10	0	0.22	0.44	0.22	0.88	304	550	304	7
13	+10	0	0.44	0	0.44	0.88	608	0	608	7
14	+10	0	0.35	0.18	0.35	0.88	483	225	483	7
15	+10	0	0.29	0.29	0.29	0.88	401	363	401	7
16	+10	0	0	0.88	0	0.88	0	1100	0	7
17	−10	0	0.22	0.44	0.22	0.88	304	550	304	7
18	−10	0	0.29	0.29	0.29	0.88	401	363	401	7
19	−10	0	0.44	0	0.44	0.88	608	0	608	7
20	−10	0	0.35	0.18	0.35	0.88	483	225	483	7
21	−10	0	0	0.88	0	0.88	0	1100	0	7
22	−20	+10	0.29	0.29	0.29	0.88	401	363	401	7

MP : Measuring Plane

ML : Measuring Line

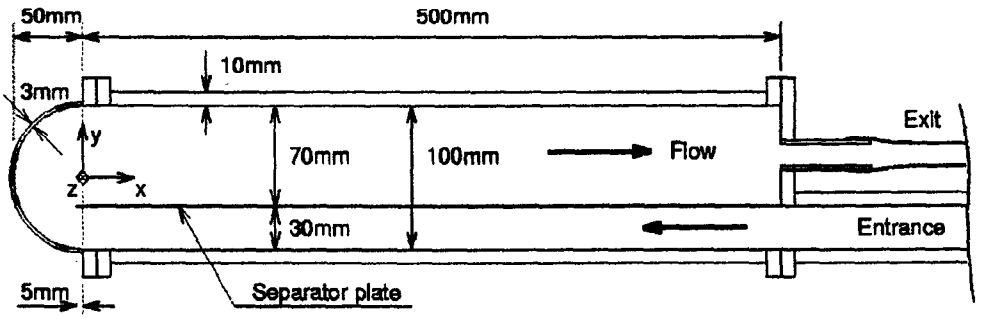

Figure 1 Test section for ESS 2D flow measurement

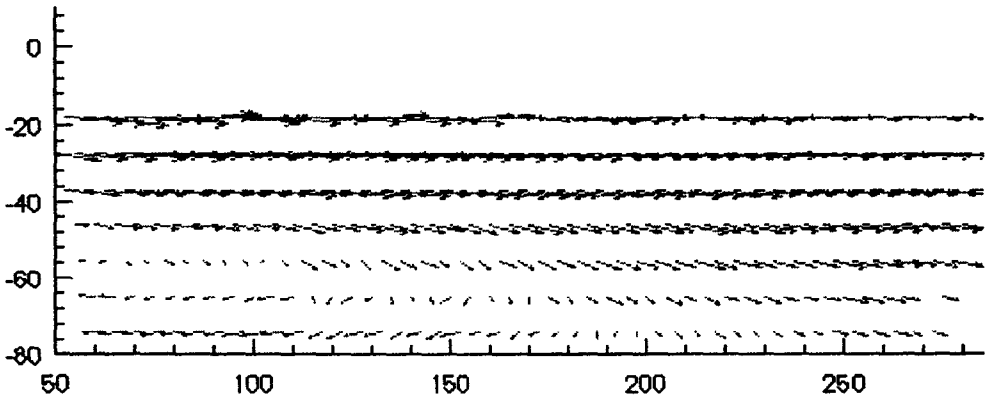

Fig.2 Time-averaged vector field (experimental) for the upper channel near the top.

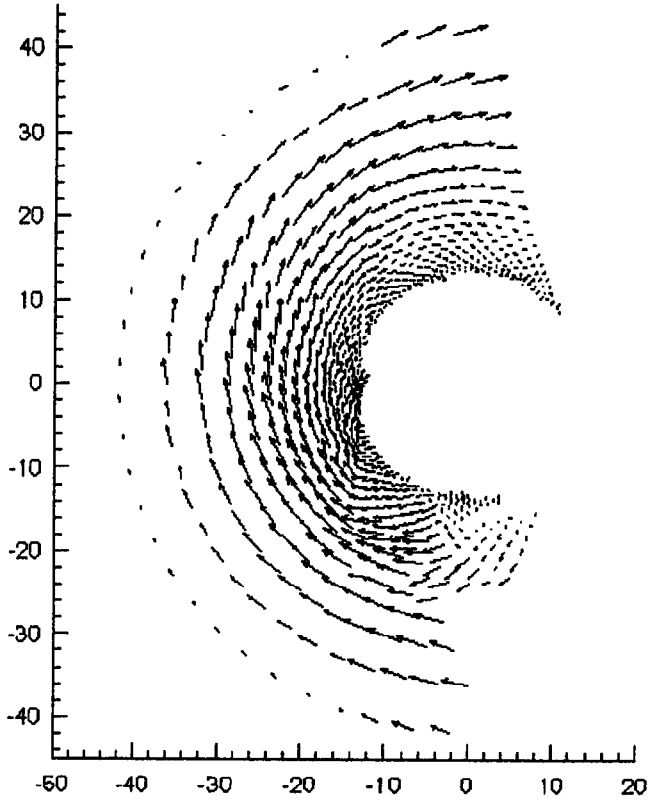

Figure 3 Time-averaged vector field for the hemicylindrical region.

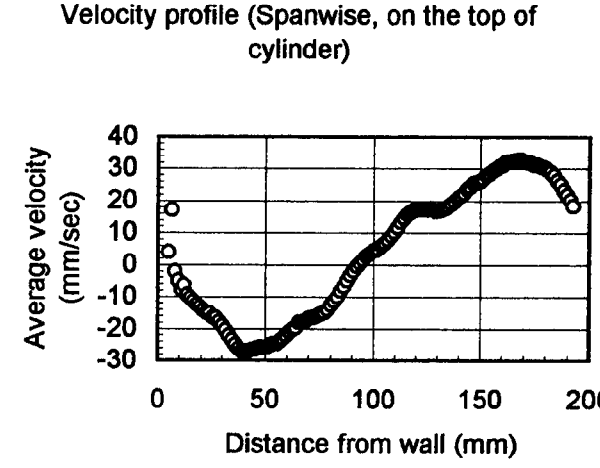

Figure 4 Spanwise velocity distribution (time averaged profile)

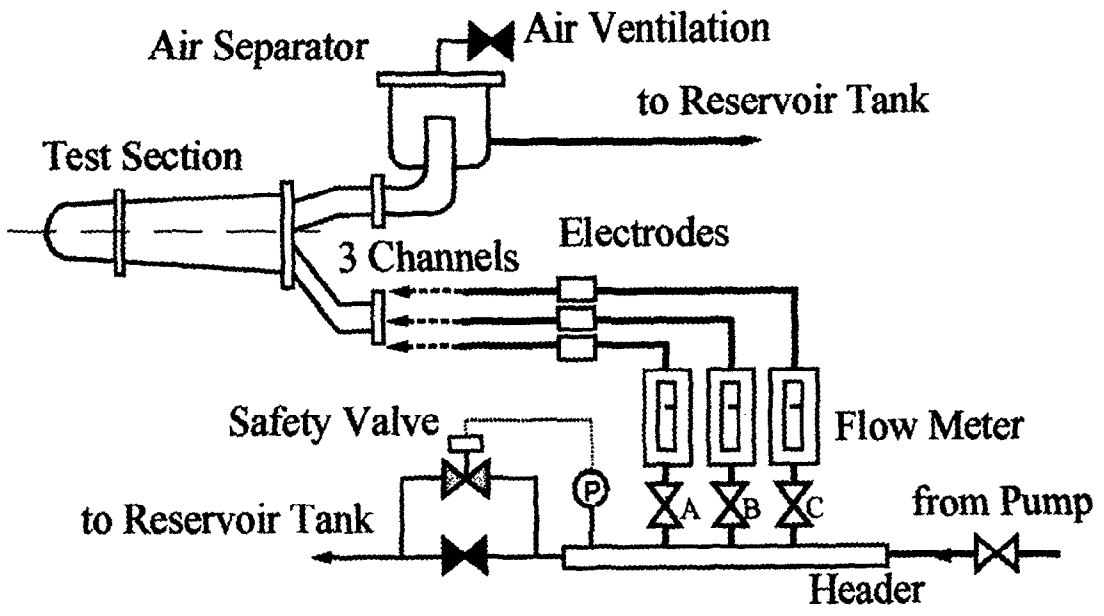

Fig. 5 Water Loop for ESS Experiment

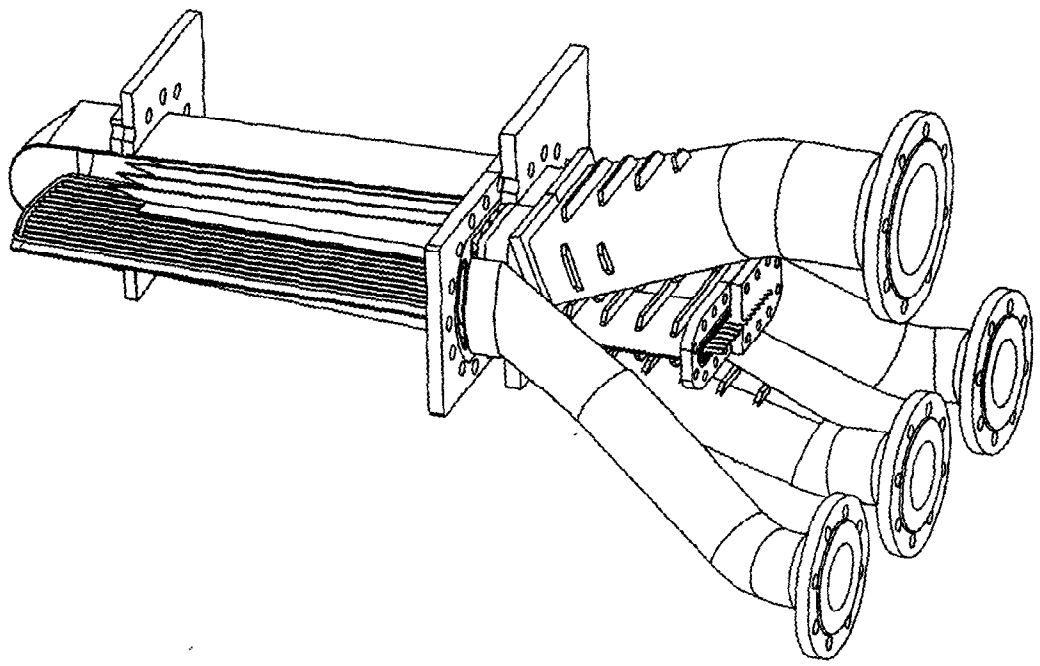

Fig. 6 Cut-out View of the ESS Model

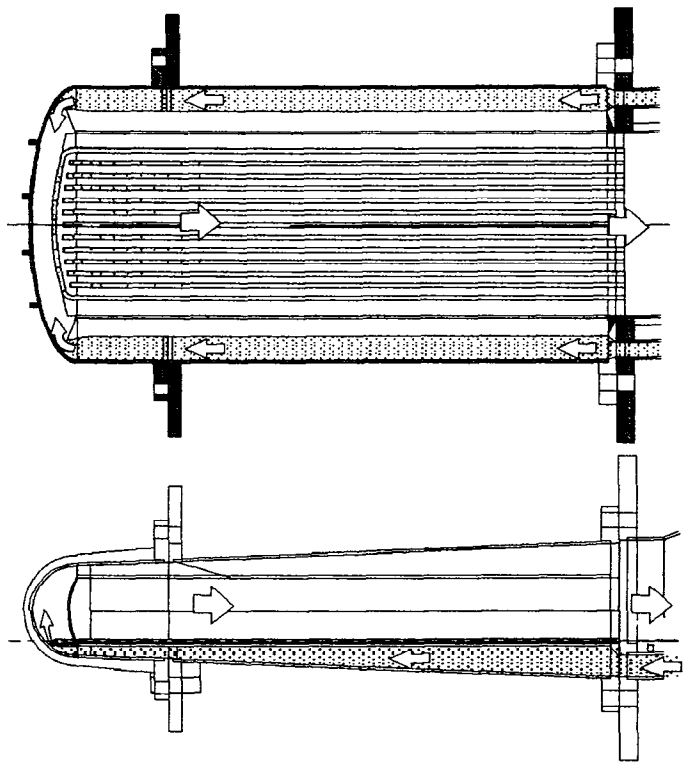

Fig.7 Flow Direction in the ESS Model

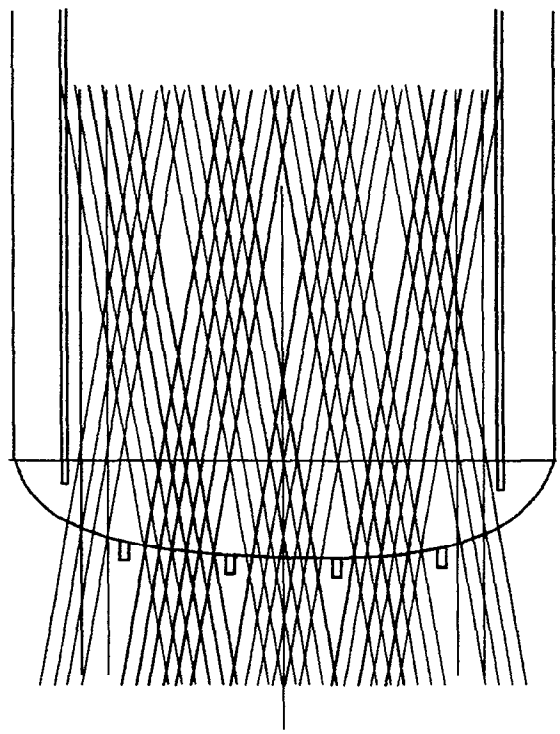

Fig.8 Arrangement of Measuring Lines for Vector Mapping

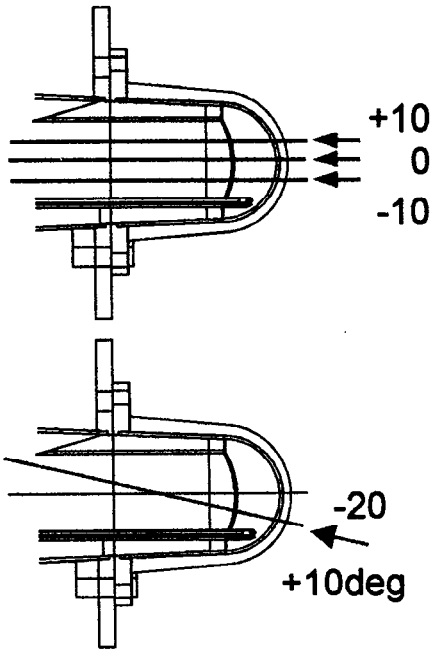

Fig.9 Position of Measuring Planes

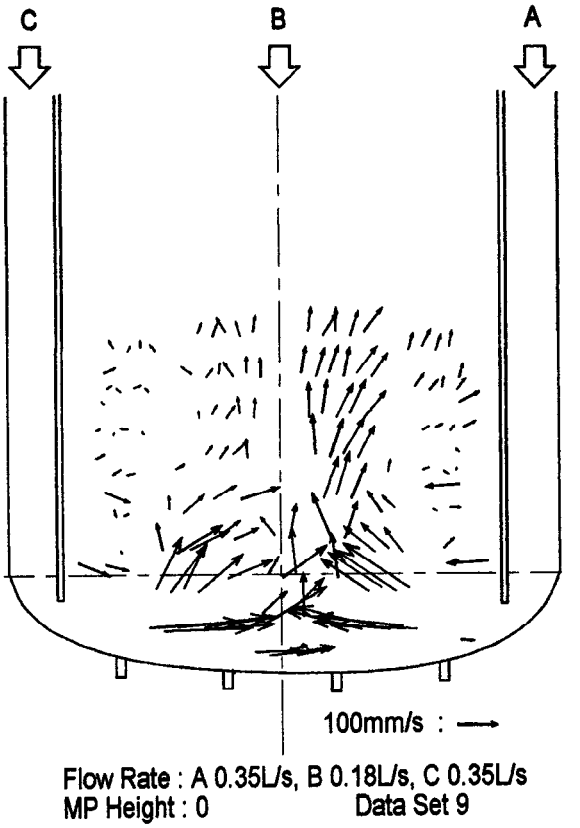

Fig.10 Vector Flow Field (2 : 1 : 2)

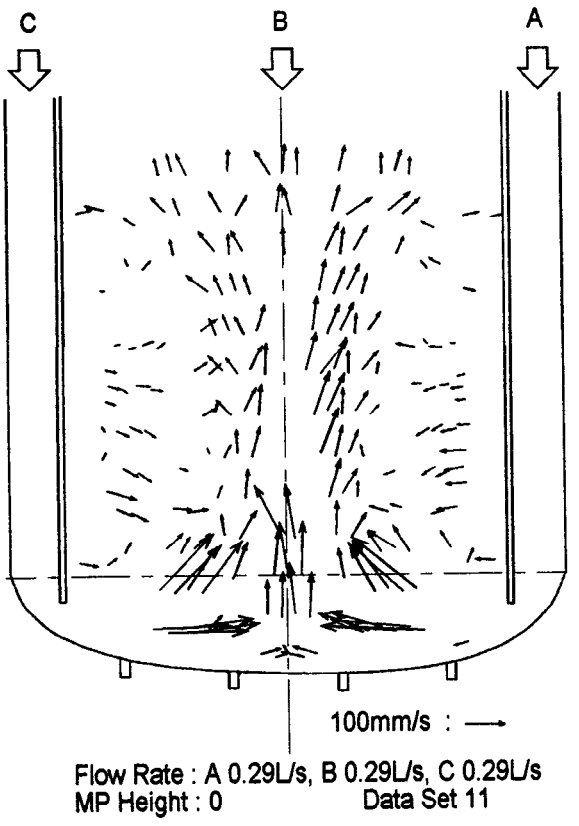

Fig.11 Vector Flow Field (1 : 1 : 1)

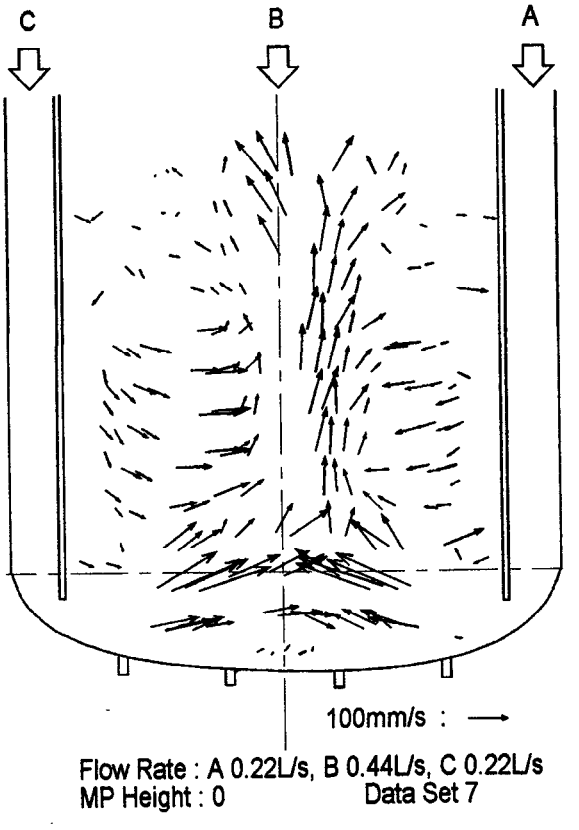

Fig. 12 Vector Flow Field (1 : 2 : 1)

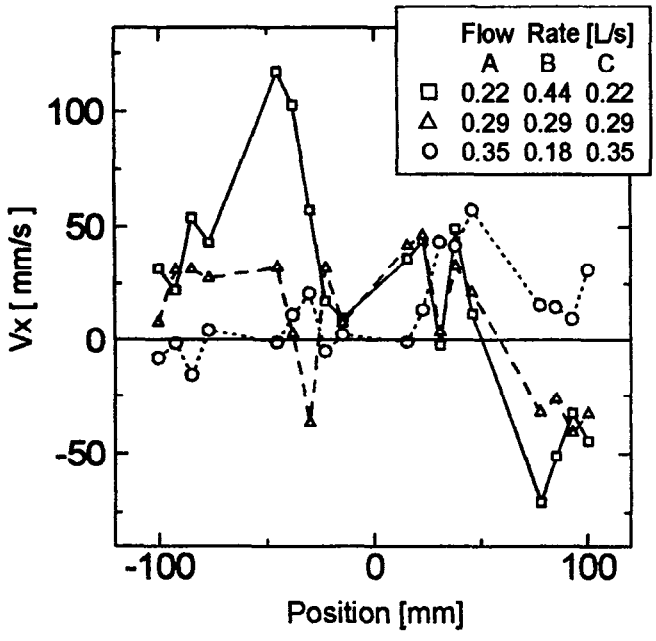

Fig. 13 Vx Profile along X Axis

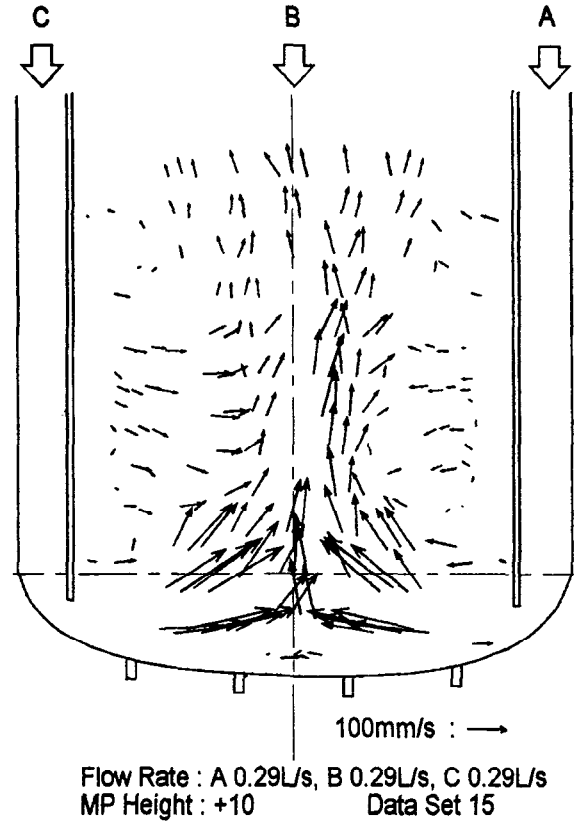

Fig.14 Vector Flow Field (1 : 1 : 1)

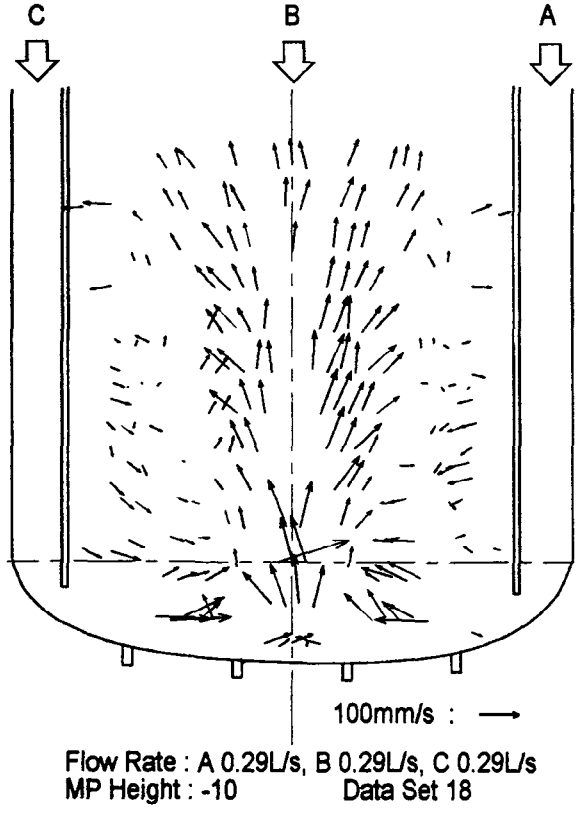

Fig.15 Vector Flow Field (1 : 1 : 1)

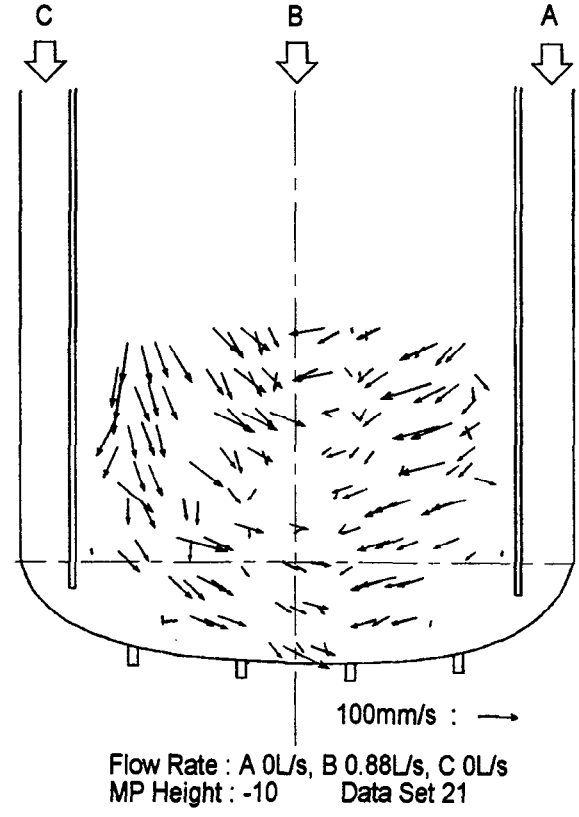

Fig.16 Vector Flow Field (0 : 1 : 0)

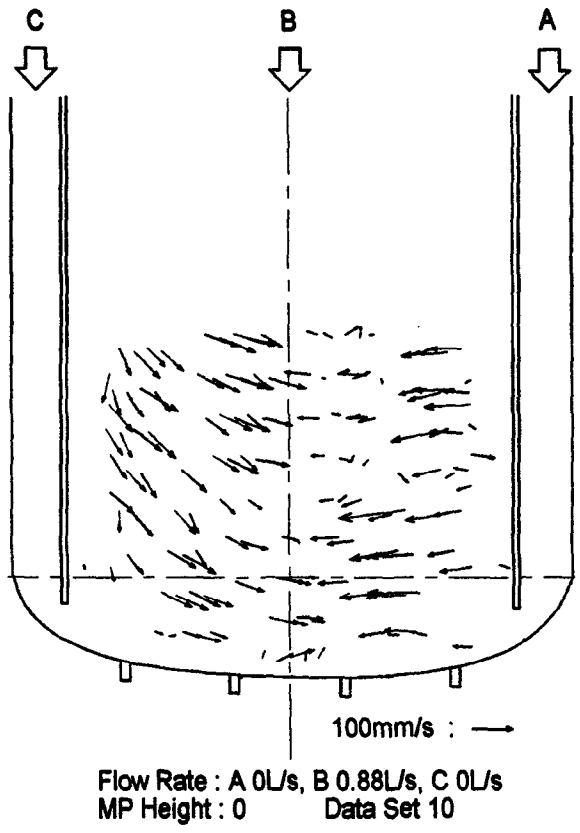

Fig. 17 Vector Flow Field (0 : 1 : 0)

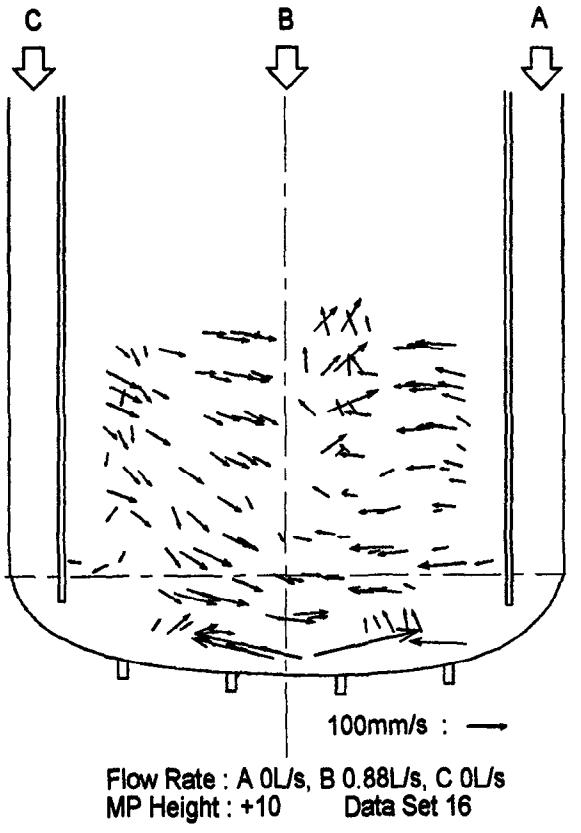

Fig. 18 Vector Flow Field (0 : 1 : 0)